

# Relationship between electrophysiology and Ca<sup>2+</sup> signalling in Goldfish intact hearts

## Abstract

Fish have become an increasingly popular model to study cardiovascular physiology given its numerous advantages. However, many studies centred on the cardiac properties of Zebrafish (*Danio rerio*) are generally done in isolated cardiomyocytes and present limitations. This review evaluates the systolic Ca<sup>2+</sup> signalling (Ca<sup>2+</sup>-T) parameters and the electrophysiological behaviour of intact Goldfish hearts, in order to establish a new fish model to study cardiovascular physiology. In this review we will discuss how Ca<sup>2+</sup> signalling and the electrophysiological performance of Goldfish intact hearts were evaluated in comparison with Zebrafish using Local Field Fluorescence Microscopy (LFFM) and sharp microelectrode recordings. The hearts were perfused through the bulbus arteriosus with the Ca<sup>2+</sup> indicator Rhod-2, among other solutions. Ventricular Action Potentials (APs) and Ca<sup>2+</sup>-T recorded from the Goldfish were considerably lengthier than those of the Zebrafish. Analysis of the Goldfish AP showed the half duration (APD<sub>50</sub>) of the ventricular AP heart was significantly longer ( $370.38 \pm 8.8$  ms) than the Zebrafish ( $83.9 \pm 9.4$  ms). Moreover, the half duration of the Ca<sup>2+</sup>-T was also much longer for Goldfish ( $266.9 \pm 7.9$  ms) than the Zebrafish ( $99.1 \pm 2.7$  ms). Blocking the L-type Ca<sup>2+</sup> channel with Nifedipine in the Goldfish shortened both the APs and Ca<sup>2+</sup>-T. The AP Duration (APD) in the Goldfish hearts shortened with increasing temperature, and not surprisingly, Ryanodine and Thapsigargin perfusion significantly reduced the amplitude of epicardial Ca<sup>2+</sup>-T and prolonged the AP duration, indicating Ca<sup>2+</sup> dependent inactivation of the L-type Ca<sup>2+</sup> channels. These data suggest the electrophysiological properties and Ca<sup>2+</sup>-T in intact Goldfish hearts are more similar to those in the human heart endocardium, especially when compared with other fish models such as the Zebrafish. The central objective of this review is to discuss the strengths of the Goldfish as a new model to study cardiac signalling, and ultimately human cardiac pathology.

**Keywords:** Intact Goldfish heart • Excitation-contraction coupling • Electrophysiology • Pulsed LFFM

## Introduction

The Zebrafish (*Danio rerio*) has become an increasingly popular model for examining heart function due to its availability, cost, and the ease at which transgenic models can be developed [1-4]. Although the Zebrafish model is extremely useful in many fields of review, the model presents several limitations [5] when used to study cardiac electrophysiology.

In this review, we examine the properties of the Goldfish (*Carassius auratus*) heart, and discuss its usefulness as an alternative experimental model to study the mechanism of excitation-contraction coupling. Goldfish hearts present many of the same advantages as the Zebrafish heart, such as its availability, the ease at which transgenic models can be developed using CRISPR/Cas9 [6], as well as being used in electrophysiological

Maedeh Bazmi<sup>1</sup>, Ariel L Escobar<sup>2\*</sup>

<sup>1</sup>Quantitative Systems Biology Program, School of Natural Sciences, University of California, Merced, CA, USA

<sup>2</sup>Department of Bioengineering, School of Engineering, University of California, Merced, CA, USA

\*Author for correspondence:

Ariel L Escobar, Department of Bioengineering, School of Engineering, University of California, Merced, CA, USA, E-mail: aescobar4@ucmerced.edu

Received date: August 19, 2021

Accepted date: September 02, 2021

Published date: September 09, 2021

and  $Ca^{2+}$  signalling experiments [7,8]. However, there are some unique advantages in the Goldfish model that are only present when compared to the Zebrafish model (Figures 1A-1J).

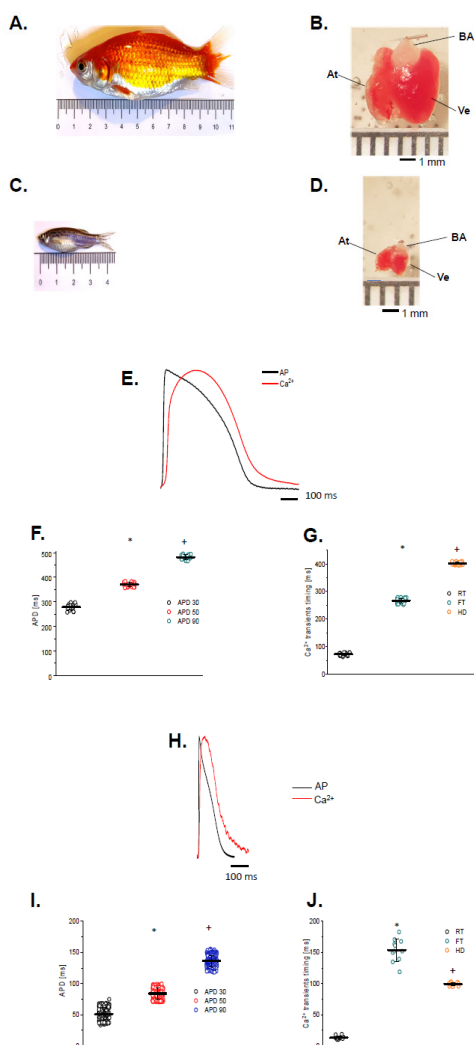


**Figure 1:** Adult Goldfish measuring roughly 9.4 mm (A); and Zebrafish measuring 3.7 mm (C); pictured for scale. Adult Goldfish hearts (B); are significantly larger than adult Zebrafish hearts (D); It is possible to observe in both Goldfish and Zebrafish hearts, the ventricle (Ve), the atrium (At), and the Bulbus Arteriosus (BA). The main characteristics of both APs and  $Ca^{2+}$ -T were recorded at 23°C in Goldfish hearts (E); and Zebrafish hearts (H); The kinetic parameters for Goldfish intact hearts, including rising time ( $72.4 \pm 4.5$  ms), fall time ( $266.9 \pm 7.9$  ms), and half duration ( $402.1 \pm 4.4$  ms) were established (G); as well as the AP durations at 30% ( $278.4 \pm 12.4$  ms), 50% ( $370.4 \pm 8.8$  ms), and 90% ( $136.2.5 \pm 9.0$  ms) repolarization (F); The kinetic parameters for Zebrafish intact hearts, including rising time ( $13.3 \pm 2.9$  ms), fall time ( $153.7 \pm 18.0$  ms), and half duration ( $99.1 \pm 2.7$  ms) were established (J); as well as the AP durations at 30% ( $51.2 \pm 10.4$  ms), 50% ( $83.9 \pm 9.4$  ms), and 90% ( $136.2.5 \pm 9.0$  ms) repolarization (I). The  $Ca^{2+}$  kinetic parameter between Goldfish and Zebrafish also changes substantially (G) and (J). The symbols \* and + indicate that the measurements are statistically significant between them. p-value<0.01.

The most notable difference between the two models is the substantially larger body and heart size of the Goldfish in comparison to the Zebrafish. Interestingly, the Goldfish heart rate [9] (109 beats/min) is closer to the heart rate in larger mammals (i.e. Dogs, Humans) when compared to the Zebrafish [5] (162-169 beats/min). Furthermore, Goldfish  $Ca^{2+}$ -T (Figures 1E and 1G) kinetic parameters (i.e., Rise Time (RT), Fall Time (FT), and Half Duration (HD)) are much slower than their counterparts in the Zebrafish (Figures 1H and 1J). The Goldfish  $Ca^{2+}$ -T present similar kinetic characteristics within canine hearts both in isolated myocytes [10] and at the intact heart level [11]. APs recorded from the Goldfish model are also significantly longer than that of Zebrafish. Kinetically, the APD90 in Goldfish is very similar to ones recorded in the endocardial ventricular layer of dog hearts [12] at similar temperatures (25°C). Although the Goldfish epicardial APs do not present a “spike and dome” behaviour [13,14], the epicardial APs in Goldfish do present a waveform strikingly similar to ones recorded from the dog endocardial layer. Finally, the Goldfish APD at 90% repolarization (APD90) is very similar to the human QT segment at similar temperatures [15].

To evaluate the main mechanisms of the Goldfish heart we evaluated APs and  $Ca^{2+}$ -T. Many vertebrates permeate  $Ca^{2+}$  into their myocytes through L-Type  $Ca^{2+}$  channels. More specifically, the role of the L-type  $Ca^{2+}$  currents in the excitability and contractility, the contribution of SR  $Ca^{2+}$  release to  $Ca^{2+}$ -T, and the repolarization of the AP were examined in this review. These goals were tackled using a combination of LFFM [14-16] and microelectrode intracellular recordings [10,11,16]. The results presented here show the Goldfish to have epicardial Action Potentials (APs) duration and kinetics compatible with endocardial APs of larger mammals such as humans or dogs. The influx of  $Ca^{2+}$  through L- type  $Ca^{2+}$  channels not only define the duration of AP but may also be the key trigger for  $Ca^{2+}$  release from the SR. In addition, Goldfish hearts have a similar AP temperature [17,18] and heart rate dependency [19,20] to that of larger mammals.

Like in other vertebrates, the fish heart needs to increase its heart rate to cope with environmental stress conditions and to handle the metabolic demands of its skeletal muscle. As poikilotherm vertebrates, the internal temperature of a fish is dependent on the ambient water temperature, which can modify both the kinetics of APs and  $Ca^{2+}$ -T. In general, contractility has a larger temperature dependency than excitability, possibly due to the temperature dependency of the ATP hydrolysis needed to pump  $Ca^{2+}$  back into the SR.

Although there are numerous advantages to any fish model, it is important to clarify there are significant structural differences

between mammals and fish. Perhaps the most important features may be the two-chambered heart and the absence of the T-tubule system in the fish ventricular myocyte [12,13,21]. Independently of this structural distinction, in this review, we found an encouraging fact, the presence of a significant fraction of  $\text{Ca}^{2+}$  release from the SR.

An important component of  $\text{Ca}^{2+}$ -T during systole in Goldfish comes from SR  $\text{Ca}^{2+}$  release, where the fraction of SR  $\text{Ca}^{2+}$  released contributes to the amplitude of the  $\text{Ca}^{2+}$ -T, similar to larger mammals [11]. If SR  $\text{Ca}^{2+}$  release is impaired, the duration of the AP increases [16,17], suggesting  $\text{Ca}^{2+}$  dependent inactivation of the L-type  $\text{Ca}^{2+}$  channels is key to controlling the AP duration [18]. This would then suggest  $\text{Ca}^{2+}$  dependent inactivation of the L-type  $\text{Ca}^{2+}$  channel is the most likely mechanism prolonging the AP duration in the absence of  $\text{Ca}^{2+}$  release from the SR.

In conclusion, the data presented in this review suggest the Goldfish heart may be an excellent model to study physiological mechanisms at the intact heart level. Moreover, its similarities with larger mammals open a new avenue to study human physiology and pathology.

## Literature Review

### Materials and methods

• **Heart preparation:** Adult Goldfish or Zebrafish (Figures 1A and 1C) were anesthetized *via* immersion in ice-cold water containing tricaine methane-sulfonate (0.16 mg/ml) solution for 2-5 min. Tanks varying in volume were utilized respective to fish size (Figure 1). Experiments at UC Merced were performed under UC Merced animal facilities are Association for Assessment and Accreditation of Laboratory Animal Care accredited and Office of Laboratory Animal Welfare certified and fully comply with all regulations, policies, and standards that protect animal welfare. Animal use in our studies fully complied with the National Institutes of Health Guide for the Care and Use of Laboratory Animals.

Goldfish hearts (Figure 1B) were dissected, extracted, cannulated onto a gauge 27 needle, and perfused in a Langendorff system at a rate of 60  $\mu\text{L}/\text{min}$  driven by gravity. Multiple solutions including the Ringer were perfused through the bulbus arteriosus with the aid of a self-designed  $\mu$ -manifold. Zebrafish hearts (Figure 1D) were dissected, cannulated onto a gauge 32 needle, and perfused in a Langendorff system at a rate of 10  $\mu\text{L}/\text{min}$  driven by gravity through the bulbus arteriosus. The solutions contained NaCl 137 mM, KCl 5.4 mM,  $\text{CaCl}_2$  1.8 mM,  $\text{MgCl}_2$  0.5 mM, HEPES 10 mM, and glucose 5.5 mM. The  $\text{Ca}^{2+}$  dye Rhod-2 AM was perfused into the heart with a Harvard pump. The temperature of the heart

was controlled with the aid of a Peltier unit positioned in the bottom of the recording chamber and measured with a linearized semiconductor temperature sensor.

### Experimental setup

• **Optical measurements:**  $\text{Ca}^{2+}$ -T were recorded with Local Field Fluorescence Microscopy (LFFM technique) [17-19]. This technique can assess physiological parameters by exciting exogenous probes present in the tissue and detecting the light emitted by these fluorescent indicators. The excitation (532 nm Yag laser) and emitted light propagated through a multimode fiber optic (200  $\mu\text{m}$  diameter, 0.67 NA). The emitted light then travelled back through the multimode fiber, dichroic mirrors, and filters (610 nm), and was focused on an avalanche photodiode (Perkin Elmer, USA). The signal is digitized by an A/D converter (NI, USA) and acquired by a PC.

• **Electrophysiological measurements:** Epicardial electrical recordings of the APs were obtained using sharp glass microelectrodes filled with 3 M KCl, connected to a high input impedance differential amplifier (WPI, USA). Glass microelectrodes were fabricated with a 10-20 M $\Omega$  resistance [20,22]. Data were recorded with an acquisition system Digidata 1440A (Molecular Devices, Sunnyvale, CA) using pClamp 10 software. Fluorescence and membrane potential were always recorded from the ventricular epicardium. The hearts were paced with the aid of two acupuncture needles placed in the apex of the ventricle. The larger bulbus arteriosus of the Goldfish allows the heart to be cannulated with a needle gage 27, while the Zebrafish requires a gage 32-34. This minor difference in needle gage leads to significantly larger fluxes, which can lead to an increased perfusion rate of drugs during an experiment.

• **Statistical analysis:** In whole heart experiments, there are two main causes of variance. The stochastic nature of APs and  $\text{Ca}^{2+}$ -T and differences between different animals. The time constant for activation ( $\tau_{\text{on}}$ ) and the time constant for the relaxation ( $\tau_{\text{off}}$ ) of the  $\text{Ca}^{2+}$ -T were calculated as

$$\tau_{\text{on}} = RT/2.2 \text{ and } \tau_{\text{off}} = FT/2.2$$

Furthermore, the gain of  $\text{Ca}^{2+}$  induced  $\text{Ca}^{2+}$  release was calculated as The  $\text{Ca}^{2+}$ -T recorded in the presence of Ryanodine and Thapsigargin mostly represents the influx across  $\text{Ca}^{2+}$  across the plasma membrane. Thus, it is possible to calculate the gain of the  $\text{Ca}^{2+}$  induced  $\text{Ca}^{2+}$  release as

$$\text{Gain}_{\text{CICR}} = \text{Amplitude}_{\text{control}} \text{ of } \text{Ca}^{2+} / \text{Amplitude}_{\text{Ry-Th}} \text{ of } \text{Ca}^{2+}$$

The data are presented as multiple measurements (n, dot cloud)

recorded in different hearts (N) with the mean ± SEM (solid lines). Statistical significance was tested using a two-sample Kolmogorov-Smirnov test (OriginPro 2020). The difference was significant if the p-value was <0.01.

**Results**

**• General properties of Goldfish and Zebrafish excitability and contractility:** One of the more noticeable advantages of the Goldfish model may be the size of the model. Goldfish are 3 times longer and 2.7 times wider than Zebrafish (Figures 1A and 1C). Due to their larger body size, Goldfish consequently have a significantly larger ventricle than Zebrafish, being 3.7 times longer and 3 times wider (Figures 1B and 1D). As a result of larger ventricle dimensions, the volume of the ventricle is 34 times larger in the Goldfish than the Zebrafish. Another physiological advantage of the Goldfish heart is the presence of a longer ventricular action potential duration (Figures 1E and 1F) and the Ca<sup>2+</sup> transients at room temperature (23°C; Figures 1E and 1G) when compared to the Zebrafish (Figures 1H-1J). These findings suggest the Goldfish heart may be better related to the human heart than the Zebrafish.

Figure 1E shows the main characteristics of both APs and Ca<sup>2+</sup>-T recorded from the Goldfish ventricle. The AP parameters were 3 times longer for Goldfish (Figure 1F) compared to the Zebrafish (Figure 1I).

Several kinetic parameters such as RT, FT, and HD were also evaluated for the Ca<sup>2+</sup>-T in both Goldfish (Figure 1G) and Zebrafish (Figure 1J). The kinetic properties of Goldfish Ca<sup>2+</sup>-T were significantly slower (RT=72.4 ± 4.5 ms, FT=266.9 ± 7.9 ms, HD=402.1 ± 4.4 ms; n=40 measurements) than the ones recorded in Zebrafish hearts (Figure 1J) (RT=13.3 ± 2.9 ms, FT=153.7 ± 18.0 ms, and HD=99.1 ± 2.7 ms; n=11 measurements).

**• Role of L-type Ca<sup>2+</sup> currents in the excitability and contractility of Goldfish hearts:** Experiments presented in Figure 2, address the contribution of the L-type Ca<sup>2+</sup> current to the ventricular AP kinetics and the amplitude of Ca<sup>2+</sup>-T. Partially blocking the L-type Ca<sup>2+</sup> current with 10 μM Nifedipine (Figure 2A) significantly reduced all parameters that define the duration of the epicardial AP (APD30 reduced from 278.4 ± 12.4 ms to 210.31 ± 12.84 ms, APD50 reduced from 370.3 ± 8.8 ms to 283.6 ± 8.0 ms, and APD90 reduced from 481.5 ± 9.5 ms to 389.5 ± 16.9 ms; (Figures 2B-2D), respectively; n=25 measurements) indicating the L-type Ca<sup>2+</sup> is partially responsible for the duration of phase 2 during the AP.

Furthermore, Nifedipine significantly reduced the amplitude of Ca<sup>2+</sup>-T by 40% (from 0.84 ± 0.06, n=84 measurements to 0.49 ± 0.04, n=106 measurements; (Figures 2E and 2F)). To compare

the kinetics of the Ca<sup>2+</sup>-T before and after 10 μM Nifedipine perfusion, the control and experimental traces were normalized to their maximum amplitude (Figure 2G). Interestingly, there was a significant reduction in the RT and HD of the Ca<sup>2+</sup> transients (RT; from 72.4 ± 4.5 ms, n=40 measurements to 57.7 ± 5.1 ms, n=22 measurements; (Figures 2H and 2J), respectively), suggesting a shorter APD30 reduced the duration of the Ca<sup>2+</sup> influx through L-type Ca<sup>2+</sup> channels. However, the FT of the Ca<sup>2+</sup> transients did not change significantly after Nifedipine perfusion (Figure 2I; from 266.9 ± 7.9 ms; n=40 measurements to 269.0 ± 12.9 ms; n=22 measurements), even after the normalization of the Ca<sup>2+</sup>-T before and after Nifedipine (Figures 2G and 2I).

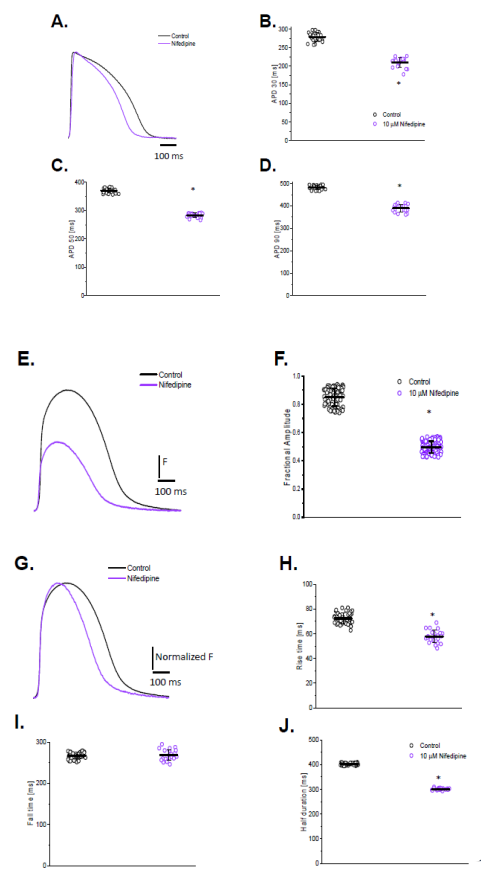


**Figure 2:** Perfusion with 10 μM Nifedipine lead to a significant decrease in the action potential duration at 30% (278.4 ± 12.4 ms to 210.31 ± 12.84 ms), 50% (370.3 ± 8.8 ms to 283.6 ± 8.0 ms), and 90% (481.5 ± 9.5 ms to 389.5 ± 16.9 ms) repolarization (A-D); Time course of Ca<sup>2+</sup> transients in the absence and the presence of Nifedipine (E); Perfusion with 10 μM Nifedipine significantly reduced the amplitude of Ca<sup>2+</sup> transient by 40% (F); The normalized Ca<sup>2+</sup> transient recording (G); shows a significant change in the kinetics of this systolic event. Furthermore, the rise time was significantly reduced (H); from 72.4 ± 4.5 ms to 57.7 ± 5.1 ms), and half-duration of the Ca<sup>2+</sup> transients (J); from 402.1 ± 4.4 ms to 300.9 ± 3.7 ms) Although the fall time of the Ca<sup>2+</sup> transients increased from 266.9 ± 7.9 ms to 269.0 ± 12.9 ms, this change was not significant (I). The symbol \* indicates that the measurements are statistically significant between them. p-value<0.01.

• **Temperature dependency of APs and Ca<sup>2+</sup>-T in Goldfish hearts:**

Figure 3A shows a 5°C increase in the temperature significantly shortened the APD30 (Figure 3B; 212.4 ± 12.3 ms to 164.3 ± 9.9 ms), APD50 (Figure 3C; from 320.1 ± 9.5 ms to 244.1 ± 11.5 ms), and APD90 (Figure 3D; from 443.5 ± 10.2 ms to 356.6 ± 5.2.5 ms; n=87 measurements) in the Goldfish. Interestingly, this is opposite to what has been previously observed in the mice model and is more similar to what has previously been observed in larger mammals.

The temperature dependency of the Ca<sup>2+</sup>-T is presented in Figure 3E. The Goldfish Ca<sup>2+</sup>-T became smaller (from 0.82 ± 0.01, n=107 measurements to 0.33 ± 0.01, n=107 measurements;

Figures 3E and 3F) and faster (Figures 3E and 3G) after increasing the Goldfish heart temperature by 5°C. The differences in the kinetics can be better observed in Figure 3G, where the Ca<sup>2+</sup>-T traces were normalized. The smaller Ca<sup>2+</sup>-T amplitude illustrated in Figure 3E can be explained due to a shorter AP duration at higher temperatures. Particularly, all the kinetic parameters were significantly faster at higher temperatures (RT decreased from 25.0 ± 0.6 ms at 23.5°C to 19.25 ± 1.47 ms at 28.5°C; FT decreased from 334.1 ± 6.5 ms at 23.5°C to 271.0 ± 11.1 ms at 28.5°C; HD reduced from 382.6 ± 2.9 ms at 23.5°C to 308.0 ± 4.8 ms at 28.5°C; n=110 measurements at 23°C and n=120 measurements at 28.5°C; Figures 3H-3J, respectively).

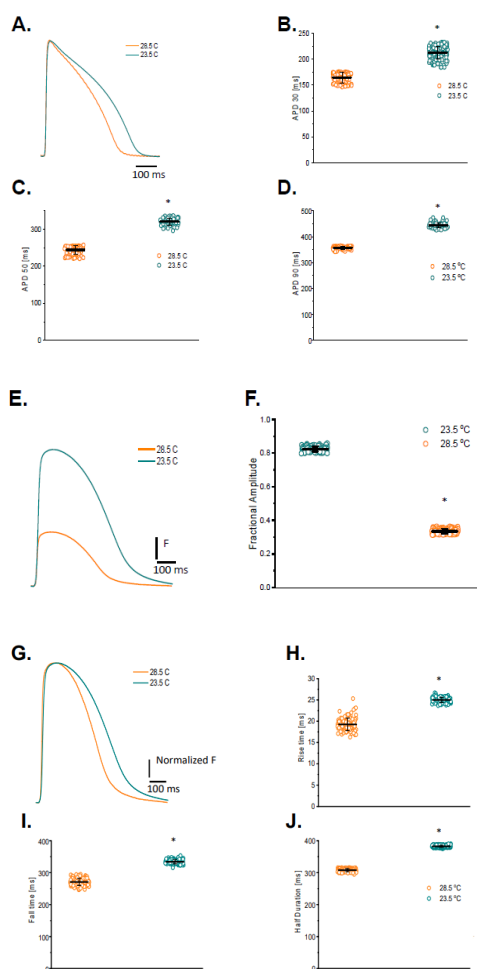


**Figure 3:** Effects of increasing the temperature from 23.5°C to 28.5°C on AP transient (A); The increased temperature shortened the AP duration at AP duration 30% (B); from 212.4 ± 12.3 ms to 164.3 ± 9.9 ms), 50% (C); from 320.1 ± 9.5 ms to 244.1 ± 11.5 ms), and 90% repolarization (D); from 443.5 ± 10.2 ms to 356.6 ± 5.2.5 ms). The increase in temperature also leads to shorter and smaller Ca<sup>2+</sup>-T (E); The effect of temperature on the amplitude of the Ca<sup>2+</sup>-T is illustrated in panel (F); Moreover, to better observe the changes in the kinetics of the Ca<sup>2+</sup>-T traces, they were normalized (G); The global increase in temperature of the heart reduced the rise time (H); from 25.0 ± 0.6 ms at 23.5°C to 19.25 ± 1.47 ms at 28.5°C), fall time (I); from 334.1 ± 6.5 ms at 23.5°C to 271.0 ± 11.1 ms at 28.5°C), and half duration (J); from 382.6 ± 2.9 ms at 23.5°C to 308.0 ± 4.8 ms at 28.5°C of Ca<sup>2+</sup>-T. The symbol \* indicates that the measurements are statistically significant between them. p-value<0.01.

• **Heart rate dependency of APs and Ca<sup>2+</sup>-T:** Modifications to the APs and Ca<sup>2+</sup>-T in response to an increased heart rate are presented in Figure 4. The time courses of APs as a function of the heart rate are presented in Figure 4A illustrates how an increase in heart rate significantly reduces APD30, APD50, and APD90 (Figures 4B-4D respectively). It is likely the AP duration was reduced because the L-type Ca<sup>2+</sup> channels did not recover from inactivation. Figure 4E shows how the amplitude of the Ca<sup>2+</sup>-T decreases as a function of the heart rate. The amplitude of the Ca<sup>2+</sup>-T as a function of the heart rate shows a statistically significant negative staircase behavior (Figure 4F). To evaluate how the heart rate changed the kinetics of the Ca<sup>2+</sup>-T, the traces shown in Figure 4E were normalized by their maximum amplitude (Figure 4G). Figure 4G indicates that not only the amplitude of the transient decreased but also the kinetics of this systolic event exhibit a strong change in its kinetic behavior compared to 1.2 Hz. Figures 4H-4J depict how the fractional amplitude, RT, FT, and HD of the Ca<sup>2+</sup>-T became smaller as a function of the heart rate.

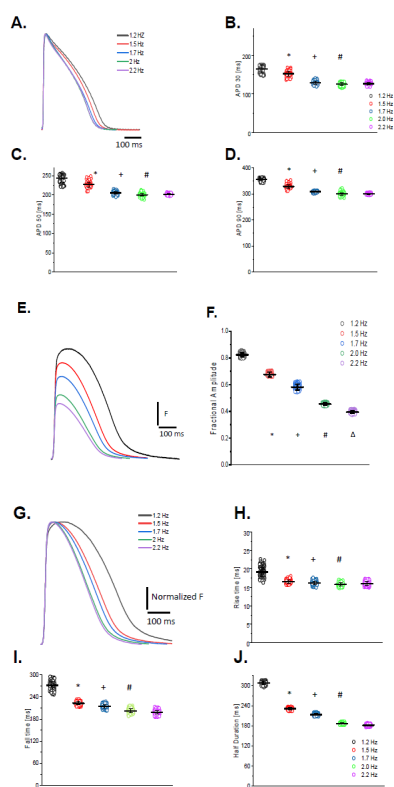


**Figure 4:** Time courses of APs and Ca<sup>2+</sup>-T as a function of the heart rate (A); As the heart rate increases, the duration of the APs at 30% (B); 50% (C); and 90% (D); repolarization gets shorter. The amplitude of the Ca<sup>2+</sup>-T decreased (E); in a step staircase manner as a function of the heart rate (F); The kinetics of this systolic event experiment a strong change in its kinetic behavior that is better observed in the amplitude of the Ca<sup>2+</sup>-T were normalized (G); specifically, there was a reduction in the rise time (H); fall time (I); and the half duration (J); of the Ca<sup>2+</sup>-T as a function of heart rate. The symbols \*, # and Δ indicate that the measurements are statistically significant between two consecutive heart rates. p-value < 0.01.

• **Contribution of SR Ca<sup>2+</sup> release to Ca<sup>2+</sup>-T and the repolarization of the AP:** The calculated Gain<sub>CICR</sub> was 2.25 ± 0.06 for the Goldfish heart. Figures 5A and 5B show that in Goldfish hearts, there is a significant amount of SR Ca<sup>2+</sup> release. Interestingly, the inhibition of Ca<sup>2+</sup> released from the SR also modified the repolarization of the ventricular AP. Figures 5C-5F show APs recorded at 23°C. The most likely hypothesis is that the AP gets longer because of the decrease of the Ca<sup>2+</sup> dependent inactivation produced by the SR Ca<sup>2+</sup> release. Interestingly, the Ryanodine and Thapsigargin effect we see in the Goldfish heart is very similar to the effects observed by other authors in dog hearts where the attenuation of Ca<sup>2+</sup> release mediated by BAPTA also prolonged the AP [23].

The prolongation of the AP duration by Ryanodine and Thapsigargin was observed in Goldfish ventricular APs recorded at 23°C (Figures 5A-5C). Ryanodine and Thapsigargin still prolonged the AP duration at all the levels (Figures 5D-5F).

## Discussion

### Comparison between Goldfish hearts and other vertebrates

Goldfish hearts and body size are noticeably larger than that of Zebrafish (Figures 1A-1D), which immensely aids in successful dissection and extraction of a healthy intact heart. Due to this immense difference in physical size, Goldfish also have longer APs (Figure 1E) than the Zebrafish (Figures 1H and 1I). Interestingly, although the Goldfish lack a classical “spike and dome” behavior [13,14, 21], the APD90 in Goldfish (Figure 1F) is very similar to ones recorded in the endocardial ventricular layer of canine hearts [24] at a similar temperature (25°C). Even more, the Goldfish Ca<sup>2+</sup>-T present similar kinetic characteristics (Figures 1E and 1G) within canine hearts both in isolated myocytes [10] and at the intact heart level [11], something that is not observed for the Zebrafish (Figures 1H and 1J).

This is significant because the canine model has historically been the classic model to study human cardiac electrophysiology, as they are strikingly similar to one another.

### Role of the L-type Ca<sup>2+</sup> channels in excitability and contractility of the Goldfish heart

In most vertebrate species, the influx of Ca<sup>2+</sup> through the L-type Ca<sup>2+</sup> channel is critical in defining the time course of APs and is the main mechanism to trigger ventricular Ca<sup>2+</sup> release. Results presented in Figure 2 depict the role of L-type Ca<sup>2+</sup> currents in Goldfish excitability and its ability to activate the excitation-contraction coupling process.

Partially blocking the L-type Ca<sup>2+</sup> current with 10 μM Nifedipine

[24] (Figure 2A) significantly reduced all parameters that define the duration of the epicardial AP (APD30 reduced from  $278.4 \pm 12.4$  ms to  $210.31 \pm 12.8.4$  ms, APD50 reduced from  $370.3 \pm 8.8$  ms to  $283.6 \pm 8.0$  ms, and APD90 reduced from  $481.5 \pm 9.5$  ms to  $389.5 \pm 16.9$  ms; Figures 2B-2D, respectively; n=25 measurements) indicating the L-type  $\text{Ca}^{2+}$  is partially responsible for the duration of phase 2 during the AP.

One consequence of having a decrease in the influx of  $\text{Ca}^{2+}$  is a reduction in contractility. The results presented in Figures 2E-2J demonstrates not only is the  $\text{Ca}^{2+}$  transient attenuated during systole, but there is also a change in the kinetic behavior of the  $\text{Ca}^{2+}$ -T. Previous studies have reported Nifedipine reduces the amplitude of  $\text{Ca}^{2+}$  in some fish models [13,25,26] but there is no evidence of  $\text{Ca}^{2+}$ -T shortening. However, the shortening in the half duration of the  $\text{Ca}^{2+}$ -T is observed in several mammalian models [9,16], which is very encouraging. The observed shortening in the half duration of the  $\text{Ca}^{2+}$ -T (Figures 2G-2J) is likely due to the shortening of the AP duration (Figures 2A-2D).

#### **Temperature dependency of APs and $\text{Ca}^{2+}$ -T**

Fish cannot systemically regulate their body temperature. Therefore, the temperature of the water has a big influence on the physiological behavior of the animal's cardiac function [27]. Figure 3 shows both the time course of the AP and  $\text{Ca}^{2+}$ -T display a significant temperature dependency. Interestingly, the depolarization of the AP has a much lower temperature dependency than the repolarization (Figures 3A-3D). The repolarization can include multiple events that can be regulated by the  $\text{Ca}^{2+}$  released from the SR. Some mechanisms include the  $\text{Ca}^{2+}$  dependent inactivation of the L-type  $\text{Ca}^{2+}$  channel. The reduction in the AP duration as a function of the temperature increase has been reported by other authors in other fish models [28-31]. However, there was no information about the  $\text{Ca}^{2+}$ -T amplitude and its temperature dependency in fish models.

Interestingly, raising the temperature by  $5^{\circ}\text{C}$  resulted in  $\text{Ca}^{2+}$ -T having smaller amplitude (Figure 3E). Moreover, the decrease in the amplitude of the  $\text{Ca}^{2+}$  transient promoted by a temperature increase was statistically significant (Figure 3F), possibly due to a shorter AP at higher temperatures (Figures 3G-3J). If the AP is shortened, the duration of the L-type  $\text{Ca}^{2+}$  current will also shorten, thus less  $\text{Ca}^{2+}$  is brought into the cell. Interestingly, this response has been reported in other mammalian species [32,33] where experiments to measure the mechanical activity in Rabbit papillary muscle describes a very similar temperatures dependency. Though the authors conclude this decrease cannot be solely related to a decrease in the duration of  $\text{Ca}^{2+}$  release, as it could also be

related to an increase in the rate of  $\text{Ca}^{2+}$  sequestration by the SR.

#### **Heart rate dependency of APs and $\text{Ca}^{2+}$ -T**

Goldfish hearts present both a frequency dependency of the AP duration (Figures 4A-4D) and a negative staircase behavior of  $\text{Ca}^{2+}$ -T (Figures 4E, 4F). The profile of decrease of the AP duration at the three levels (i.e., APD30, APD50, and APD90), shows a similar profile. The decrease in the AP duration as a function of the heart rate is similar to the decrease observed for mammals [10,28,29] and other fish models [34-36].

Figure 4E shows how the amplitude of the  $\text{Ca}^{2+}$ -T decreases as a function of the heart rate. The amplitude of the  $\text{Ca}^{2+}$ -T as a function of the heart rate shows a statistically significant negative staircase behavior (Figure 4F). To evaluate how the heart rate changed the kinetics of the  $\text{Ca}^{2+}$ -T, the traces shown in Figure 4E were normalized by their maximum amplitude (Figure 4G). Figure 4G indicates not only the amplitude of the transient decreased but also the kinetics of this systolic event exhibit a strong change in its kinetic behavior. Figures 4H-4J depict how the fractional amplitude, RT, FT, and HD of the  $\text{Ca}^{2+}$ -T [36] became smaller as a function of the heart rate.

Another important outcome of the heart rate dependency in Goldfish hearts is the effect on the  $\text{Ca}^{2+}$ -T amplitude (Figure 4E). Specifically, the appearance of a negative staircase behavior as the heart rate increases (Figure 4F). All the kinetic parameters such as the rise time, fall time, and half duration of the  $\text{Ca}^{2+}$ -T become faster (Figures 4G-4J). The observed changes in the kinetics of the  $\text{Ca}^{2+}$ -T have been reported for other fish models [34,37]. In terms of the negative staircase behavior of contractility, there are reports for other fish models related to a decrease in the amplitude of  $\text{Ca}^{2+}$ -T [36]. Interestingly, not all mammals present a negative staircase behavior as a function of the heart rate in the amplitude of the  $\text{Ca}^{2+}$ -T or the mechanical response. This could imply that  $\text{Ca}^{2+}$  dependent inactivation of L-type  $\text{Ca}^{2+}$  channels and a faster  $\text{Ca}^{2+}$  reloading rate of the SR play a larger role in Goldfish hearts in comparison with larger mammals.

#### **Role of intracellular $\text{Ca}^{2+}$ release on excitability and contractility**

$\text{Ca}^{2+}$  released from the SR can impact the repolarization of the AP through several mechanisms. For example, if the  $\text{Ca}^{2+}$  release from the SR is impaired, then  $\text{Ca}^{2+}$  dependent inactivation of L-type  $\text{Ca}^{2+}$  channels will shorten the APs for a larger  $\text{Ca}^{2+}$  release and will prolong the AP. On the other hand, the  $\text{Na}^{+}$ - $\text{Ca}^{2+}$  exchanger will prolong the AP for a larger  $\text{Ca}^{2+}$  release and it will shorten the AP for a decreased  $\text{Ca}^{2+}$  release. To evaluate how much the SR  $\text{Ca}^{2+}$  release contributes to the change in free myoplasmic  $\text{Ca}^{2+}$ -T in the Goldfish heart during systole,  $\text{Ca}^{2+}$  released from the SR was

abolished through perfusion with 10  $\mu\text{M}$  Ryanodine to block the Ryanodine receptors and with 2  $\mu\text{M}$  Thapsigargin to block the SERCA pump. Ryanodine and Thapsigargin not only significantly reduced the amplitude of  $\text{Ca}^{2+}$ -T (Figure 5A), but also reduced the fractional release by roughly 55% (Figure 5B; from  $1.0 \pm 0.05$ ,  $n=204$  measurements to  $0.45 \pm 0.01$ ,  $n=60$  measurements).

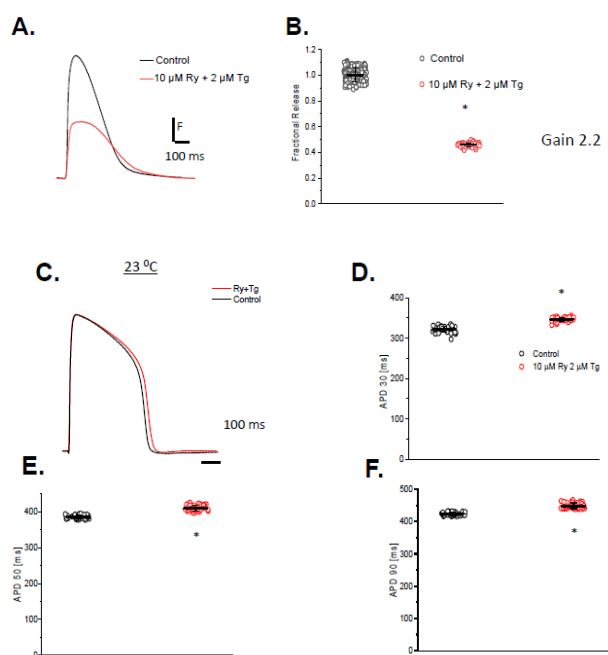


**Figure 5:** Typical  $\text{Ca}^{2+}$ -T recordings before and after perfusion of Goldfish heart with 10  $\mu\text{M}$  Ryanodine and 2  $\mu\text{M}$  Thapsigargin (A); A summary of the results illustrates a statistically significant decrease in the amplitude of  $\text{Ca}^{2+}$  transient as well as a 55% decrease in the fractional release (B); from  $1.0 \pm 0.05$  for the control condition to  $0.45 \pm 0.01$  for hearts perfused with Ryanodine and Thapsigargin. Perfusion with 10  $\mu\text{M}$  Ryanodine and 2  $\mu\text{M}$  Thapsigargin at 23°C also impaired  $\text{Ca}^{2+}$  release from the SR (C); and prolonged the duration of the AP at 30% (D); from  $321.5 \pm 7.9$  ms to  $347.1 \pm 4.9$  ms), 50% (E); increased from  $385.53 \pm 5.0$  ms to  $409.8 \pm 7.9$  ms), and 90% repolarization (F); from  $424.3 \pm 4.8$  ms to  $448.8 \pm 8.9$  ms). The symbol \* indicates that the measurements are statistically significant between them.  $p$ -value $<0.01$ .

The role of SR  $\text{Ca}^{2+}$  released as a big contributor to the systolic  $\text{Ca}^{2+}$  during the cardiac cycle strongly depends on the vertebrate species. This wide range goes from frogs that do not present  $\text{Ca}^{2+}$  release from the SR [38] to mice the  $\text{Ca}^{2+}$ -T strongly depends on the SR [9,22,27].

Figures 5A and 5B show that in Goldfish hearts, there is a significant reduction in the SR  $\text{Ca}^{2+}$  release. Interestingly, the inhibition of  $\text{Ca}^{2+}$  released from the SR also modified the repolarization of the ventricular AP. Figures 5C-5F show APs recorded at 23°C. The most likely hypothesis is that the AP gets longer because of the decrease of the  $\text{Ca}^{2+}$  dependent inactivation produced by the

decrease in the SR  $\text{Ca}^{2+}$  release [25]. Interestingly, the Ryanodine and Thapsigargin effect we see in the Goldfish heart is very similar to the effects observed by other authors in dog hearts where the attenuation of  $\text{Ca}^{2+}$  release mediated by BAPTA also prolonged the AP [23].

The prolongation of the AP duration by Ryanodine and Thapsigargin was observed in Goldfish ventricular APs recorded at 23°C. Although APs are longer at a lower temperature (Figure 5C), Ryanodine and Thapsigargin still prolonged the AP duration at all the levels (APD30 from  $321.5 \pm 7.9$  ms,  $n=40$  measurements to  $347.1 \pm 4.9$  ms,  $n=40$  measurements; APD50 from  $385.53 \pm 5.0$  ms,  $n=40$  measurements to  $409.8 \pm 7.9$  ms,  $n=40$  measurements; and APD90 from  $424.3 \pm 4.8$  ms,  $n=40$  measurements to  $448.8 \pm 8.9$  ms,  $n=40$  measurements; (Figures 5D-5F), respectively).

## Conclusion

Goldfish heart presents several physiological attributes to make it a good choice to study physiological and pathophysiological problems present in larger mammals, similar to humans. All these factors open the window for the Goldfish heart to be used to assess human cardiac function during health and disease.

## Acknowledgements

We want to thank Dr. Alicia Mattiazzi and Dr. Josefina Ramos-Franco for reviewing this review. We also want to thank Dr. Chih-Wen Ni for providing us with the Zebrafish used in this review. Supported by NIH (R01 R01GM132753 and NIH 1R01HL152296 to ALE).

## Conflict of Interest

The authors declare that the review was conducted in the absence of any commercial or financial relationships that could be construed as a potential conflict of interest.

## Author Contributions

MB, ALE designed the review; MB, ALE performed the review; MB, ALE analyzed data; and MB, ALE wrote the review.

## References

- Huttner IG, Trivedi G, Jacoby A, et al. A transgenic zebrafish model of a human cardiac sodium channel mutation exhibits bradycardia, conduction-system abnormalities and early death. *J Mol Cell Cardiol.* 61: 123-32 (2013).
- Serbanovic-Canic J, de Luca A, Warboys C, et al. Zebrafish model for functional screening of flow-responsive genes. *Arterioscler Thromb Vasc Biol.* 37(1): 130-43 (2017).
- Konantz J, Antos CL. Reverse genetic morpholino approach using cardiac ventricular injection to transfect multiple difficult-to-target tissues in the zebrafish larva. *J Vis Exp.* 88: 51595 (2014).

4. Chopra SS, Stroud DM, Watanabe H, et al. Voltage-gated sodium channels are required for heart development in zebrafish. *Circ Res.* 106(8): 1342-50 (2010).
5. Ling L, Genge CE, Cua M, et al. Functional assessment of cardiac responses of adult zebrafish (*Danio Rerio*) to acute and chronic temperature change using high-resolution echocardiography. *PLoS One.* 11(1): e0145163 (2016).
6. Fanqian Y, Liu W, Chai J, et al. CRISPR/Cas9 application for gene copy fate survey of polyploid vertebrates. *Front Genet.* 9: 260 (2018).
7. Jerri C, Zhu JX, Wilson I, et al. Cardioprotective effects of K ATP channel activation during hypoxia in goldfish *Carassius auratus*. *J Exp Biol.* 208(Pt 14): 2765-72 (2005).
8. Serena L, Gattuso A, Mazza R, et al. Cardiac influence of the  $\beta$ 3-adrenoceptor in the goldfish (*Carassius auratus*): A protective role under hypoxia? *J Exp Biol.* 222(Pt 19): jeb211334 (2019).
9. Ferreira EO, Anttila K, Farrell AP. Thermal optima and tolerance in the eurythermic goldfish (*Carassius auratus*): Relationships between whole-animal aerobic capacity and maximum heart rate. *Physiol Biochem Zool.* 87(5): 599-611 (2014).
10. Marcela F, Petrosky AD, Escobar AL. Intracellular  $Ca^{2+}$  release underlies the development of phase 2 in mouse ventricular action potentials. *Am J Physiol Heart Circ Physiol.* 302(5): H1160-1172 (2012).
11. Alarcón MML, de Yurre AR, Felice JI, Emiliano Medei, and Ariel L. Escobar. Phase 1 repolarization rate defines  $Ca^{2+}$  dynamics and contractility on intact mouse hearts. *J Gen Physiol.* 151(6): 771-85 (2019).
12. van Opbergen CJM, Koopman CD, Kok BJM, et al. Optogenetic sensors in the Zebrafish heart: A novel in vivo electrophysiological tool to study cardiac arrhythmogenesis. *PLoS One.* 17(17): e0247644 (2018).
13. van Opbergen CJM, van der Voorn SM, Vos MA, et al. Cardiac  $Ca^{2+}$  signalling in Zebrafish: Translation of findings to man. *Prog Biophys Mol Biol.* 138: 45-58 (2018).
14. Mejía-Alvarez R, Manno C, Villalba-Galea CA, et al. Pulsed local-field fluorescence microscopy: A new approach for measuring cellular signals in the beating heart. *Pflügers Arch.* 445 (6): 747-58 (2003).
15. Escobar AL, Ribeiro-Costa R, Villalba-Galea C, et al. Developmental changes of intracellular  $Ca^{2+}$  transients in beating rat hearts. *Am J Physiol Heart Circ Physiol.* 286 (3): H971-978 (2004).
16. Aguilar-Sanchez Y, Fainstein D, Mejia-Alvarez R, et al. Local field fluorescence microscopy: Imaging cellular signals in intact hearts. *J Vis Exp.* 121: 55202 (2017).
17. Antzelevitch C, Sicouri S, Litovsky SH, et al. Heterogeneity within the ventricular wall. Electrophysiology and pharmacology of epicardial, endocardial, and M cells. *Circ Res.* 69(6): 1427-49 (1991).
18. Gurabi Z, Koncz I, Patocskaï B, et al. Cellular mechanism underlying hypothermia-induced ventricular tachycardia/ventricular fibrillation in the setting of early repolarization and the protective effect of quinidine, cilostazol, and milrinone. *Circ Arrhythm Electrophysiol.* 7(1): 134-42 (2014).
19. Burashnikov A, Antzelevitch C. Acceleration-induced action potential prolongation and early afterdepolarizations. *J Cardiovasc Electrophysiol.* 9(9): 934-48 (1998).
20. Krishnan SC, Antzelevitch C. Sodium channel block produces opposite electrophysiological effects in canine ventricular epicardium and endocardium. *Circ Res.* 69(2): 277-91 (1991).
21. Vornanen M, Shiels HA, Farrell AP. Plasticity of excitation-contraction coupling in fish cardiac myocytes. *Comp Biochem Physiol A Mol Integr Physiol.* 132(4): 827-46 (2002).
22. Belevych A, Kubalova Z, Terentyev D, et al. Enhanced ryanodine receptor-mediated calcium leak determines reduced sarcoplasmic reticulum calcium content in chronic canine heart failure. *Biophys J.* 93(11): 4083-92 (2007).
23. Balázs H, Vácz K, Hegyi B, et al. Sarcolemmal  $Ca^{2+}$ -entry through L-type  $Ca^{2+}$  channels controls the profile of  $Ca^{2+}$ -activated  $Cl^{-}$  current in canine ventricular myocytes. *J Mol Cell Cardiol.* 97: 125-39 (2016).
24. Horackova M. Excitation-contraction coupling in isolated adult ventricular myocytes from the rat, dog, and rabbit: Effects of various inotropic interventions in the presence of ryanodine. *Can J Physiol Pharmacol.* 64(12): 1473-83 (1986).
25. Maedeh B, Escobar AL. How  $Ca^{2+}$  influx is attenuated in the heart during a "fight or flight" response. *J Gen Physiol.* 151(6): 722-26 (2019).
26. Bovo E, Dvornikov AV, Mazurek SR, et al. Mechanisms of  $Ca^{2+}$  handling in Zebrafish ventricular myocytes. *Pflügers Arch.* 465(12): 1775-84 (2013).
27. Piktel JS, Jeyaraj D, Said TH, et al. Enhanced dispersion of repolarization explains increased arrhythmogenesis in severe versus therapeutic hypothermia. *Circ Arrhythm Electrophysiol.* 4(1): 79-86 (2011).
28. Litovsky SH, Antzelevitch C. Rate dependence of action potential duration and refractoriness in canine ventricular endocardium differs from that of epicardium: Role of the transient outward current. *J Am Coll Cardiol.* 14(4): 1053-66 (1989).
29. Lukas A, Antzelevitch C. Differences in the electrophysiological response of canine ventricular epicardium and endocardium to ischemia. Role of the transient outward current. *Circulation.* 88(6): 2903-15 (1993).
30. Yan GX, Antzelevitch C. Cellular basis for the electrocardiographic J wave. *Circulation.* 93(2): 372-79 (1996).
31. Bjørnstad HE, Sager MG, Refsum H. Effect of bretylium tosylate on ventricular fibrillation threshold during hypothermia in dogs. *Am J Emerg Med.* 12(4): 407-12 (1994).
32. Belevych AE, Terentyev D, Terentyeva R, et al. The relationship between arrhythmogenesis and impaired contractility in heart failure: role of altered ryanodine receptor function. *Cardiovasc Res.* 90(3): 493-502 (2011).
33. Laurita KR, Katta R, Wible B, et al. Transmural heterogeneity of calcium handling in canine. *Circ Res.* 92(6): 668-75 (2003).
34. Maylie J, Morad M. Evaluation of T- and L-type  $Ca^{2+}$  currents in shark ventricular myocytes. *Am J Physiol.* 269(5 Pt 2): H1695-1703 (1995).
35. Petros N, Wettwer E, Christ T, et al. Adult Zebrafish heart as a model for human heart? An electrophysiological study. *J Mol Cell Cardiol.* 48(1): 161-71 (2010).
36. Ramos-Franco J, Aguilar-Sanchez Y, Escobar AL. Intact heart loose patch photolysis reveals ionic current kinetics during ventricular action potentials. *Circ Res.* 118(2): 203-15 (2016).
37. Lin E, Craig C, Lamothe M, et al. Construction and use of a Zebrafish heart voltage and calcium optical mapping system, with integrated electrocardiogram and programmable electrical stimulation. *Am J Physiol Regul Integr Comp Physiol.* 308(9): R755-768 (2015).
38. Baláti B, Varró A, Papp JG. Comparison of the cellular electrophysiological characteristics of canine left ventricular epicardium, M cells, endocardium and Purkinje fibres. *Acta Physiol Scand.* 164(2): 181-90 (1998).